The Alkali Molten Globule State of Ferrocytochrome *c*: Extraordinary Stability, Persistent Structure, and Constrained Overall Dynamics†

D. Krishna Rao, Rajesh Kumar, M. Yadaiah, and Abani K. Bhuyan*

School of Chemistry, University of Hyderabad, Hyderabad 500046, India

Received September 15, 2005; Revised Manuscript Received January 3, 2006

ABSTRACT: This paper describes the structural and dynamic properties of a hitherto uncovered alkali molten globule (MG) state of horse "ferrocytochrome *c*" (ferrocyt *c*). Several experimental difficulties mainly because of heme autoxidation and extraordinary stability of ferrocyt *c* have been overcome by working with the carbonmonoxide-bound molecule under extremely basic condition (pH 13) in a strictly anaerobic atmosphere. Structural and molecular properties extracted from basic spectroscopic experiments suggest that cations drive the base-denatured CO-liganded protein to the MG state. The stability of this state is ∼5.2 kcal mol^{-1}, and the guanidinium-induced unfolding transition is sharp ($m_g \sim 2.3$ kcal mol^{-1} M^{-1}), suggesting contents of rigid tertiary structure. Strategic experiments involving the measurement of the CO association rate to the base-denatured protein and intrachain diffusion rates measured by laser photolysis of CO indicate a substantially restricted overall motion and stiffness of the polypeptide chain in the MG state. Possible placement of the state in the folding coordinate of ferrocyt *c* is discussed.

During the past 30 years or so, a large volume of literature has most definitely indicated the existence of the molten globule (MG)[1] state, which, viewing from the classical perspective of protein folding, has been referred to as the third thermodynamic state of proteins; the native and unfolded states are the other two (*1*). The concept of the MG state emerged at a time when the view of the two-state nature of folding of small globular proteins (*2*−*4*) had appeared to break down. "Compact molecular states containing nativelike secondary structure" were temporally resolved in the early stages of folding of an increasingly large set of proteins (*5*−*7*). These intermediate folding structures appeared to fit nearly flawlessly into the molecular organizational definition of the classic MG state (*1*) and thus provided the basis to propose that the MG state corresponds to early kinetic intermediates in protein folding. Several concerns arise, however. How can the unfolded chain achieve so nativelike structural organization so early, in perhaps the submillisecond regime? Where along the reaction coordinate is the folding transition-state poised? Does the transition from the unfolded to the MG state involve a rate-limiting barrier-crossing event? About the same time, theoretical and computer simulation studies of protein folding detected ensembles of MG-like structures that occur very late in the folding course (*8*). It is now generally accepted that the MG state, characterized by the presence of nativelike secondary structure and molecular compactness but lacking both nativelike side-chain packing and solvation of the partially hydrophobic core, corresponds to late folding intermediates (*9*−*11*).

While the classic MG state was detected in anion-containing acid medium (*12*), stabilization under diverse solvent conditions of equilibrium states of proteins that broadly meet with the definition of the MG state has been reported in due course (for example, see refs *1, 13*−*16*). These developments raise the issue of the importance of the MG-like states in the protein-folding problem. It is thus necessary to not only look at different aspect of their structure, dynamics, and molecular organization but also locate their positions in the folding coordinate.

The acid MG state is known for numerous proteins, particularly well-known for ferricytochrome *c* (ferricyt *c*) (*12*). The complementary alkali state has however been reported for only a few proteins, including β-lactamase (*17*) and barstar (*18*). Many reports on the nature of the alkaline transition and the properties of the alkali-unfolded state of ferricyt *c* have appeared (*19*−*25*), but the alkali MG state remained elusive.

Being aware of the extraordinary native-state stability and apparent two-state fast folding of the reduced form of horse cytochrome *c* (cyt *c*) (*26*−*28*), we were interested to know if a MG-like state exists for this oxidation state of cyt *c*. There are experimental difficulties though, particularly because of the enhanced autoxidation rate of the ferrous heme in acid solutions. To counter this problem and suppress the excessive stability of the protein, we test-tube-engineered the protein by liganding the ferrous heme iron with extrinsically added CO at pH 13. Under these conditions, the reduced state of cyt *c* [to be called ferrocytochrome *c* (ferrocyt *c*)

† Funds for this research were provided by the Departments of Biotechnology (BRB/15/227/2001) and Science and Technology (4/1/2003-SF) and University Grants Commission (UPE Funding), Government of India.

* To whom correspondence should be addressed: E-mail: akbsc@uohyd.ernet.in. Telephone: 91-40-2313-4810. Fax: 91-40-2301-2460.

[1] Abbreviations: GdnHCl, guanidine hydrochloride; cyt *c*, cytochrome *c*; ferricyt *c*, ferricytochrome *c*; ferrocyt *c*, ferrocytochrome *c*; cyt-CO, carbonmonoxide-bound ferrocytochrome *c*; MG, molten globule; ΔG°_D, Gibbs energy of denaturation in the absence of the denaturant; m_g, protein surface area associated with the denaturant unfolding transition; U_A and U_B states, acid- and alkali-denatured states, respectively; A and B states, acid and alkali MG states, respectively.

10.1021/bi051882n CCC: $33.50
Published on Web 02/15/2006

henceforth] is fully denatured. Upon addition of cations to the medium, the protein undergoes a transition to the MG state as judged from spectroscopic signatures. We have specifically looked into the aspects of tertiary structural organization, folding stability, and the dynamic nature of the alkali MG state by employing a set of strategic experiments. Very interestingly, the properties observed are atypical of the MG state, although the basic requirements of the definition are met. The relevance of the alkali MG state to the folding problem of ferrocyt *c* is discussed.

MATERIALS AND METHODS

Cyt *c* from Sigma (type VI) was used without further purification. Sodium dithionite was from Merck. All experiments were done in controlled anaerobic atmosphere at 22 °C.

Equilibrium Unfolding and NaCl Titration Studies. For pH unfolding studies, an 8 μM solution of cyt *c*, prepared in an aqueous medium containing 10 mM each of Tris, disodium hydrogen phosphate, and CAPS (3-[cyclohexylamino]-1-propanesulfonic acid), was titrated to different pH values in the 7−13.25 range by the use of NaOH. The titration did not upset the uniformity of the protein concentration in the samples. Samples were deaerated by using nitrogen or argon gas and reduced by adding a small volume of freshly prepared dithionite to obtain a final concentration of 2−3 mM. The samples were then incubated for ∼30 min under 1 atm CO gas pressure in tightly capped cuvettes or glass tubes. Fluorescence emission spectra (excitation at 280 nm) were taken in a FluoroMax-3 instrument (Jobin-Yvon, Horiba). Optical absorption spectra were recorded in a Cary 100 instrument. The pH titration curves were analyzed using the following transformed Henderson−Hasselbalch equation

$$y = \frac{c_u + c_f[10^{n(pH-c_m)}]}{1 + 10^{n(pH-c_m)}} \quad (1)$$

where c_u and c_f are normalized fluorescence signals for the unfolded and refolded states, respectively, n is the number of OH^- titrated, and c_m is the pH midpoint for the transition. The procedure for guanidine hydrochloride (GdnHCl)-induced unfolding experiments, where the pH was held constant at 12.9 (±0.1) by using NaOH, was the same as described above. The data were analyzed using the two-state equation (*29*).

NaCl titration studies were carried out with protein solutions (6−8 μM) prepared in NaOH containing the salt in the 0−1.5 M range. pH of the solutions were adjusted to 12.9 (±0.1). Protein reduction and CO ligation were carried out using the protocol detailed above. CD spectra were taken in a JASCO J-710 spectropolarimeter using 1 mm cuvettes.

NMR Spectroscopy. NaCl-containing D_2O solutions of 2 mM cyt *c*, the backbone amides of which were pre-exchanged, were adjusted to the pH-meter reading of 12.9 (±0.1) by adding NaOD. Protein solutions contained in NMR tubes were reduced by adding solid sodium dithionite (20 mM) under nitrogen. A gentle stream of CO was bubbled into the solutions. The tubes were then sealed with sleeved rubber stoppers and equilibrated at 22 °C for ∼30 min. Spectra were taken at 22 °C in a 400 MHz Bruker spectrometer (AV400). A 90° pulse length was calibrated for each concentration of salt used. For phase-sensitive NOESY spectra (τ_m = 150 ms), 512 t_1 were used. The spectral width was 7184 Hz.

Kinetic Measurements of the Association of CO. The procedure for these measurements has been described earlier (*30*, *31*). Briefly, cyt *c* (1 mM) dissolved in aqueous NaOH at pH 12.9 (±0.1) is deaerated and reduced by adding sodium dithionite (2 mM). A total of 25 μL of this ferrocyt *c* solution is mixed rapidly with 2 mL of NaOH solution containing 2 mM dithionite, a given amount of NaCl, and 1 mM CO. Association kinetics of CO are followed at 550 nm (dead time ∼ 5 s) at a peltier-controlled temperature of 22 °C in a Cary 100 spectrophotometer.

Laser Photolysis and Microsecond Measurements. Cyt *c* solutions (15 μM), prepared in aqueous NaOH containing NaCl in the 0−1 M range at pH 12.9 (±0.1), were deaerated and reduced by the addition of 2 mM sodium dithionite and were incubated for ∼15 min at 22 °C under 1 atm CO gas pressure in 1-cm square quartz cuvettes. CO photolysis was achieved by irradiation with 45 (±10) mJ pulses of the second harmonic output (532 nm) of a Spectra Physics Q-switched Nd:YAG laser (10 Hz). Spectral changes following each photolysis pulse were recorded with a pulsed Xe lamp. The monochromator was set to 421.5 nm. The basic configuration of the instrument is based on the Applied Photophysics laser flash photolysis spectrometer. The sample temperature was maintained by using an external circulating water bath.

RESULTS

NaCl-Induced Resistance toward Alkali Denaturation of Carbonmonoxide-Bound Ferrocytochrome c (*Cyt-CO*). Because low pH enhances autoxidation of the ferrous heme, experiments with ferrocyt *c* are best performed at a neutral to alkaline range of pH. We therefore chose to work under highly basic pH conditions in which a MG-like state of ferrocyt *c* could possibly be found. However, because of its extraordinary stability, ferrocyt *c* does not denature even in extreme alkaline conditions unless CO is allowed to bind to the ferrous heme (*32*). Figure 1a shows fluorescence-monitored base titrations of cyt-CO in the absence and presence of 0.03, 0.1, and 1 M NaCl. In saltless medium, the titration is nearly complete at pH 13. The fit to the data by the use of eq 1 indicates that three OH^- are titrated. The titration curve clearly shifts toward higher pH values as NaCl is included incrementally; in the presence of 1 M NaCl, hardly any sign of denaturation appears within the limit of achievable pH. This suggests that cations increase the stability of the protein under conditions fully denaturing otherwise.

Alkali-Denatured Cyt-CO and Its Molecular Compaction in the Presence of NaCl. Fluorescence emission intensity because of the lone tryptophan (W59) provides a reliable marker for the molecular compactness of cyt *c*. Native cyt *c* is fluorescence-silent because of excitation energy transfer from W59 to the heme (*33*). Unfolding results in an increase in the heme−tryptophan distance because of molecular expansion and, hence, a dramatic increase in the fluorescence quantum yield (*33*, *34*). The emission spectra in Figure 1b provide a number of important information. (1) The emission λ_{max} values for the GdnHCl-unfolded protein at pH 7 (called

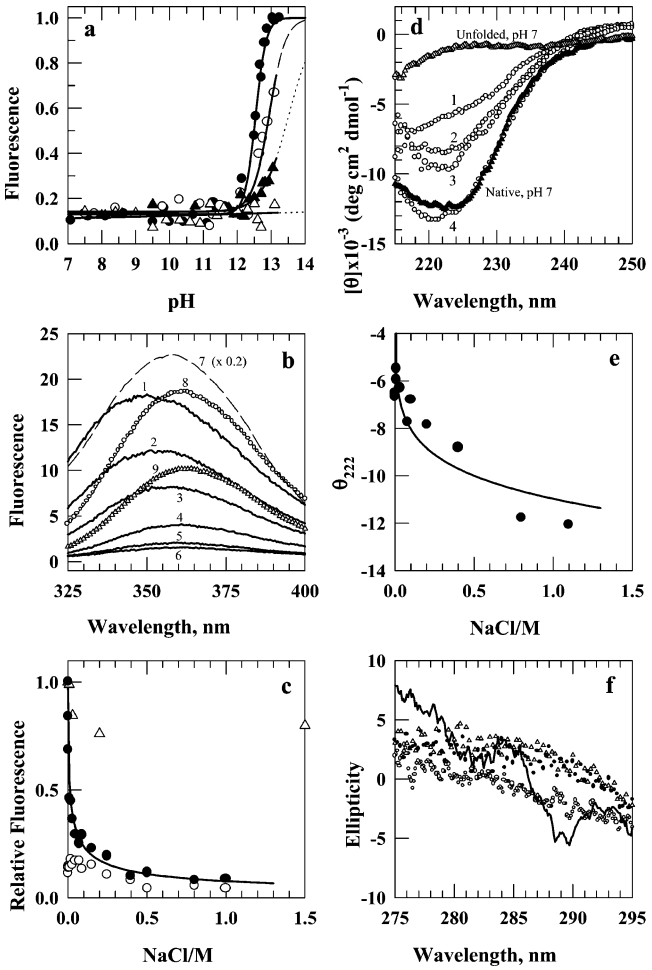

FIGURE 1: Basic results indicating cation-induced transformation of base-unfolded cyt-CO into the MG state. (a) Alkaline pH-induced unfolding of cyt-CO at 22 °C: (●) no salt, (○) in 30 mM NaCl, (▲) in 0.1 M NaCl, and (△) in 1 M NaCl. (b) Fluorescence emission spectra of cyt-CO at 22 °C. NaCl concentrations and pH values are 1, 0 M at pH 13; 2, 0.005 M at pH 13; 3, 0.01 M at pH 13; 4, 0.15 M at pH 13; 5, 0.5 M at pH 13; 6, 1 M at pH 13; 7, 0 M at pH 6.3 and 6.8 M GdnHCl (the spectrum has been scaled down 5-fold); 8, 0 M NaCl at pH 13 and 3.7 M GdnHCl; and 9, 1 M NaCl at pH 13 and 3.7 M GdnHCl. The native-state at pH 7 is fluorescence-silent. (c) Relative quenching of W59 fluorescence as a function of salt (●). In control experiments, fluorescence of ferrocyt *c* without CO ligation (○) and NATA (△) were recorded. (d) Far-UV CD spectra of cyt-CO at 22 °C. NaCl concentrations and pH values are 1, 0 M NaCl at pH 13; 2, 0.2 M NaCl at pH 13; 3, 0.4 M NaCl at pH 13; and 4, 1.1 M NaCl at pH 13. The CD spectra in the presence of high-pH GdnHCl is obscured and is not shown. (e) Variation of CD absorption at 222 nm with salt. (f) Near-UV CD spectra: cyt-CO at pH 13, 1 M NaCl, and 22 °C (○); native ferrocyt *c* at pH 7, 1 M NaCl, and 22 °C (—); unfolded ferrocyt *c* at pH 7 and 7 M GdnHCl (△); unfolded ferrocyt *c* liganded with CO at pH 7 and 7 M GdnHCl (●).

the U state, spectrum 7) and the alkali-denatured protein (called U_B state, spectrum 1) are ∼358 and 350 nm, respectively. Notice that the emission intensity at pH 13 is at least 5-fold less relative to that at pH 7. The 8-nm blue shift seen for the U_B state indicates that W59 is in a relatively apolar surrounding, shielded from water. (2) When U_B is unfolded in the presence of 3.7 M GdnHCl, the emission intensity does not change substantially (spectrum 8). However, the emission λ_{max} shifts to ∼362 nm. These observations indicate that the U_B state is maximally unfolded in terms of molecular expansion, although W59 is repositioned in a more polar water-exposed environment when an unfolding amount of GdnHCl is added to the U_B solution. (3) NaCl drives the U_B state to compactness (spectra 1−6), because the fluorescence decreases with increments of the salt. In the presence of ∼1 M NaCl, the fluorescence is nearly fully quenched, indicating the formation of the MG state. It is also clear that the emission λ_{max} shifts gradually to the right with increments of NaCl. The MG state shows a λ_{max} ∼ 358 nm, indicating that W59 in the compact protein is relatively more exposed to water. The MG state can be unfolded by the addition of GdnHCl. Spectrum 9 is obtained when the protein solution that shows spectrum 6 also contains 3.7 M GdnHCl. The λ_{max} (∼360 nm) is roughly maintained, but the fluorescence intensity increases, indicating the unfolding of the MG state.

Characteristically, the MG state is as compact as the native state (*1*). Figure 1c shows this result even more clearly: the molecular compactness of the U_B state in the presence of >0.5 M NaCl is close to that of native cyt *c*, indicating a salt-induced transition of the U_B state to the MG state.

Far-UV CD-Moniotored Seconadary Structure in the Presence of NaCl. The CD spectra in Figure 1d show secondary-structure content in the relevant protein states. At 222 nm, the molar residue ellipticity (MRE) for the GdnHCl-unfolded ferrocyt-CO is roughly −1100. The corresponding value for the U_B state is −5900, indicating that this state is not fully unfolded. A considerable residual secondary structure characterizes the alkali-denatured cyt-CO protein. With increments of NaCl, the secondary structure is strengthened. Spectra 1−4 show the changes induced by NaCl. In the presence of 1.1 M NaCl, the MRE value is comparable with that for the native protein at pH 7, suggesting that the MG state is fully formed. Typically, far-UV CD spectra of proteins in the MG state are similar to those of the native states (*5*). The control CD spectra were recorded at pH 7, because the spectra at pH 13 are obscured when GdnHCl is added to the protein solution.

Figure 1e shows the variation of the 222-nm ellipticity with salt in the 0−1.1 M range. Clearly, cyt-CO at pH 13 acquires substantial secondary structure in the presence of >0.5 M NaCl, suggesting a transformation of the U_B state to the MG state.

Absence of Near-UV CD Signal. MGs are generally distinguished by a dramatic loss of near-UV CD signal (*1*, *35*). Figure 1f compares the aromatic CD signals of native ferrocyt *c* and base-denatured cyt-CO in the presence of 1 M NaCl. The 282- and 290-nm bands of native ferrocyt *c* (pH 7 and 1 M NaCl) that arise from the coupling of the electric transition dipole moments of the W59 indole and the heme are not traceable in the salt-containing alkaline medium (pH 13 and 1 M NaCl), apparently indicating some loosening of the tertiary structure. A comparison of this spectrum with those for the GdnHCl-unfolded protein at pH 7 (see the caption of Figure 1) indicates some content of the tertiary structure in the MG state. It does not however necessarily mean an increased fluctuation and conformational averaging for the W59 side chain (see the Discussion).

NMR Spectral Features of Alkali-Denatured Cyt-CO in the Presence of NaCl. Increased internal mobility and side-chain environmental averaging, a documented characteristic of the MG state, is better checked by ^{1}H NMR (*12*, *36*). Ferrocyt *c* as such is native at pH 13, and the NMR lines are narrow and well-dispersed (Figure 2a). Upon addition

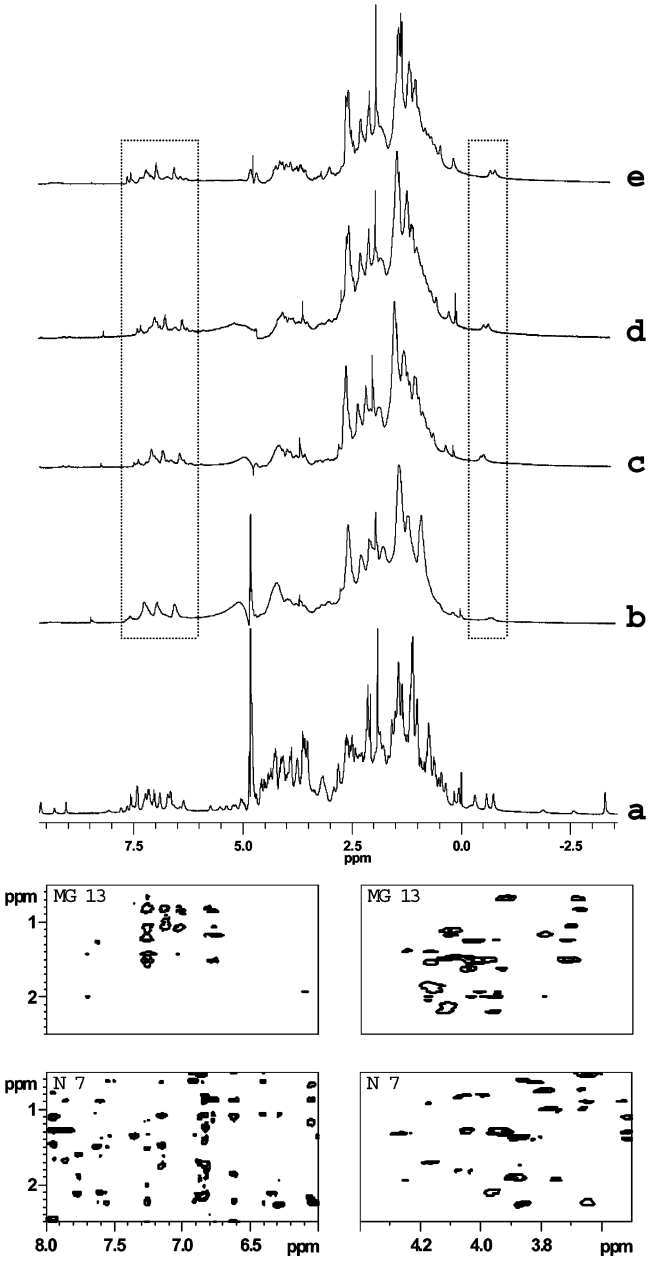

FIGURE 2: NMR spectra (400 MHz). (a) Native state of ferrocyt *c* at pH 13 with no salt. (b) Unfolded cyt-CO at pH 13 with no salt. (c) Cyt-CO at pH 13 with 0.02 M NaCl. (d) Cyt-CO at pH 13 with 0.5 M NaCl. (e) Cyt-CO at pH 13 with 1 M NaCl. Changes in the spectrum with increments of NaCl are seen in both aliphatic and aromatic regions. Boxed regions in b−e highlight the progressive increase in signal dispersion. The boxed panels at the bottom show sections of phase-sensitive NOESY spectra showing interactions involving aliphatics and aliphatic−aromatic side chains in native ferrocyt *c* at pH 7 (N 7) and in the MG state of cyt-CO at pH 13 with 1 M NaCl (MG 13). All spectra were taken at 22 °C.

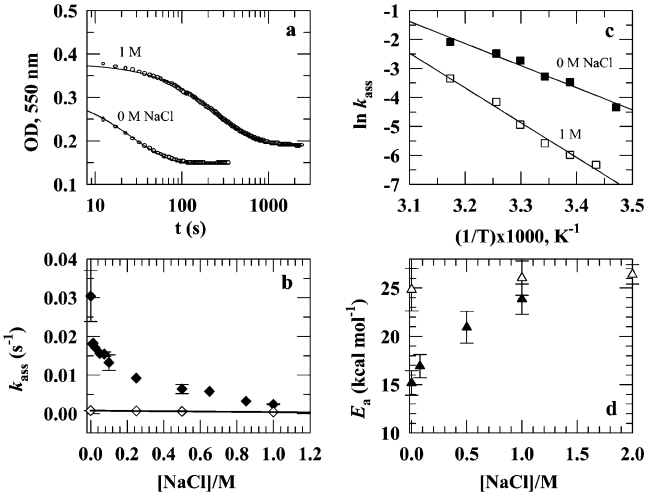

FIGURE 3: Results for the CO association reaction, cyt *c* + CO → cyt-CO monitored by 550-nm heme absorbance. (a) Representative kinetic traces showing the influence of NaCl on the CO association rate at pH 13. (b) NaCl dependence of the association rate constant, k_{ass}, at pH 13 (◆). In the control experiment, the dependence of k_{ass} on NaCl was measured for native ferrocyt *c* at pH 7 with 0.5 M GdnHCl (◇). (c) Arrhenius plots for the CO association reaction at pH 13. (d) Dependence of the activation energy, E_a, for CO association reactions on the concentration of NaCl at pH 13 (▲) and pH 7 with 0.5 M GdnHCl (△).

of CO to the same solution under identical conditions, the protein unfolds as indicated by the loss of both chemical-shift dispersion and line shape (Figure 2b). When NaCl is included in the unfolded protein solution, the spectrum appears to regain partly both dispersion and sharpness of resonances all over the spectral width (parts c−e of Figure 2). This result is inconsistent with the generic observation that the NMR spectra of the MG and unfolded states are similar (*37*−*39*). Line broadening of the resonances, associated characteristically with the MG state (*40*), is not seen either. The spectra presented show that the MG state being interrogated here carries reasonable traces of rigid tertiary structure involving both aliphatic and aromatic side chains.

Sections of phase-sensitive NOESY spectra presented at the bottom of Figure 2 (pH 13 and 1 M NaCl) substantiate the claim. A good number of long-range NOE interactions involving aliphatic side chains (bottom right of Figure 2) and aliphatic and aromatic side chains (bottom left of Figure 2) indicate the presence of considerable tertiary structure.

Charge Screening by Na^+ Ions Also Leads to Dynamic Constraints: A General Effect. In terms of internal mobility, the MG state exhibits increased fluctuations of the side chains relative to that in the native state (*37*, *41*), although the overall motional freedom is restrained when compared with the dynamics of the denatured state held in the absence of the stabilizing counterions. To show how the charge-screening effect of counterions generally reduces the fluctuations of groups of atoms, we conducted experiments involving kinetics of the association of CO with ferrocyt *c* at pH 13 in the presence of a variable concentration of NaCl. The rationale of the experiment is the following. Destabilized ferrocyt *c* binds CO when the latter is used in a saturating concentration (≈1 mM) (*42*, *43*). Because intramolecular thermal collisions provide the energy for barrier crossing in the association reaction, cyt + CO → cyt-CO, the rate coefficient for the reaction (k_{ass}) is expected to decrease if the amplitudes of thermal fluctuations are reduced as a result of constraints on the collective modes of intramolecular motion (*30*, *31*). The association kinetics are slow and can be conveniently measured by monitoring the absorbance at 550 nm, following the addition of a small volume of the protein solution to a CO-saturated aqueous alkali solution containing the salt.

The two representative traces for single-phase CO association kinetics shown in Figure 3a indicate that the association rate is much slower in the presence of 1 M NaCl

relative to that in the absence of the salt. Figure 3b shows the variation of the association rate coefficient, k_{ass}, with a molar concentration of NaCl. Also plotted is the NaCl-dependent variation of k_{ass} for native ferrocyt *c* in the presence of 0.5 M GdnHCl at pH 7. Clearly, the internal dynamics of alkaline ferrocyt *c* is substantially constrained relative to that of the initial state in the absence of salt. It is important to note that the experiment described here monitors the salt-induced constraints in the internal motion of the alkaline ferrocyt *c* only and not the MG state, because it is not until CO binds that the MG forms at pH 13.

From the temperature dependence of a series of association reactions (Figure 3c), we determined the activation enthalpy ($H \approx E_a$) for CO association at different concentrations of NaCl in the 0−1 M range (Figure 3d). Expectedly, E_a for CO association to the alkali-denatured state of cyt *c* increases with the salt concentration and approaches the value measured for the nativelike protein at pH 7. We attribute this to reduced motional freedom of the charge-shielded alkaline ferrocyt *c*. In terms of internal dynamics, the charge-screened state closely matches the native state. Thus, the reduced mobility is a consequence of reduced charge−charge repulsion.

Intrapolypeptide Diffusion Rates Measured by Laser Photolysis of CO. When CO is photolyzed from cyt-CO, the side chains of the histidine and methionine residues (H26, H33, M65, and M80) make transient contacts with the heme iron via the vacant coordination site of the ferrous iron until CO rebinds from the solvent (*32*, *44*). Binding of an intrapolypeptide ligand, say M, to the heme involves first diffusive motions of the two contacting sites at a rate of k_{+M} to produce a heme−ligand contact loop, the two ends of which are provided by the side chains of H18, which persists as an axial ligand, and M. The side chain of the contacting residue M can now form a bond with the heme iron or diffuse away at a rate of k_{-M}. The intrapolypeptide (or unimolecular) diffusion rate of the contacting sites in a random-coil configuration depends upon the mean-squared distance between them (*45*). Thus, the rate(s) of heme−ligand contact formation measured by flash photolysis of CO can provide information about polypeptide compaction or expansion.

Figure 4a presents a typical trace showing the observed changes in 421.5-nm absorbance in the 53 ns−45 μs time window after CO photolysis in the presence of 10 mM NaCl. The CO rebinding that sets in after ∼50 μs is not of interest here. Hence, data were acquired only up to 50 μs and were analyzed by two-exponential fits. According to previous studies (*46*, *32*), the fast and slow phases (λ_1 and λ_2, respectively) are assigned to transient binding of methionines (M80 and M65) and histidines (H26 and H33) to the heme iron of the photoproduct.

Figure 4b shows the NaCl dependence of the two observed rate constants. In a two-state approximation, $\lambda_1 = k_{+M} + k_{-M}$ and $\lambda_2 = k_{+H} + k_{-H}$, where the subscripts M and H refer to methionines and histidines, respectively. On the basis of our previous observation that the ratios k_{-M}/k_{+M} and k_{-H}/k_{+H} do not vary considerably in the 0−1 M range of GdnHCl at pH 13 (*32*), we assume that they are not strongly dependent upon the concentration range of NaCl used here either. Thus, $\lambda_1 \sim c_1 k_{+M}$ and $\lambda_2 \sim c_2 k_{+H}$, where c_1 and c_2 are constants. The NaCl dependences of λ_1 and λ_2 should then provide qualitative estimates of the distance between two intrachain

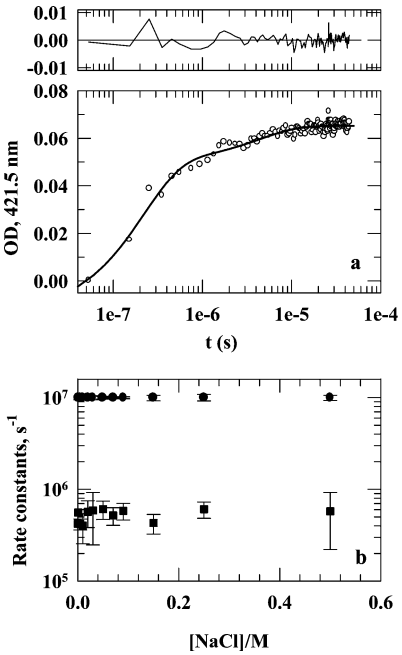

FIGURE 4: Laser photolysis experiments for the measurement of intrapolypeptide diffusion rates. (a) Typical microsecond relaxation processes observed by heme optical absorption following photolysis of CO from cyt-CO at pH 13 and 22 °C. The trace shown is for 10 mM NaCl. The kinetics are described by two relaxations of time constants ∼0.25 and ∼4 μs. (b) Indifference of both rate constants on the NaCl concentration: the two phases are due to transient binding of methionines, M65 and M80 (●), and histidines, H26 and H33 (■).

residues that make contact by diffusion. The data in Figure 4b indicate that both λ_1 and λ_2 respond little to the presence of NaCl in the 0−0.5 M range, apparently suggesting that the distances of separation of the ligands from H18 are the same in the unfolded and MG states. This might seem inconsistent with the NaCl-induced molecular compaction indicated by the fluorescence results (parts b and c of Figure 1). It is possible that the polypeptide chain in the MG state is dynamically stiff with respect to the initial denatured state without salt. Chain stiffness is known to slow intrapolypeptide diffusion rates (*45*, *47*) and could possibly compensate for an increase in the diffusion rate in the compact state.

Stability of the MG State to Unfolding by GdnHCl. Encouraged by the observations of the compactness and dynamic control in the MG state, we used tryptophan fluorescence to monitor GdnHCl-induced unfolding of cyt-CO at pH 13 and 1 M NaCl. Figure 5 shows the highly cooperative transition. Because an all-or-none-type transition operates between the native and MG states of small proteins (*1*, *48*−*50*), a two-state analysis was carried out to extract the thermodynamic parameters. The fit yields of Gibbs energy of denaturation in the absence of the denaturant (ΔG°_D) = 5.2 (±1) kcal mol^{-1}. This is enormous stability, comparable to the unfolding free energy of many small proteins (*51*). Equally interesting is the magnitude of the surface area associated with the unfolding transition. The fit yields the protein surface area associated with the denaturant unfolding transition (m_g) = 2.3 (±0.6) kcal mol^{-1} M^{-1}. This value, by comparison with 2.95 (±0.28) kcal mol^{-1} M^{-1} for GdnHCl unfolding of ferrocyt *c* in the presence of CO at pH 7, indicates a large amount of solvent exposure of amino acid residues accompanying the unfolding

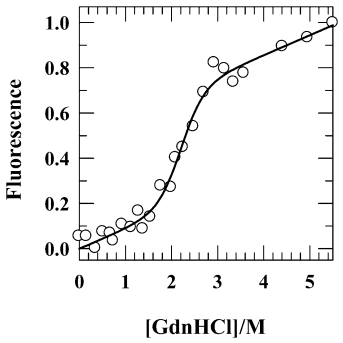

FIGURE 5: GdnHCl-induced equilibrium unfolding of cyt-CO at pH 13, 1 M NaCl, and 22 °C. The solid line is the standard two-state fit to data (*29*). The fit yields $\Delta G^{\circ}_{D} = 5.2$ (±1) kcal mol^{-1} and $m_g = 2.3$ (±0.6) kcal mol^{-1} M^{-1}.

Table 1: Properties of U_B and U_A States of Horse Cyt *c*

	U_B	U_A
fluorescence emission, λ_{max}	350 nm	356 nm
molecular expansion	equivalent to the U state	simulates the U state
peptide CD (MRE)	~5900	~3800
near-UV CD	weak	weak
^{1}H NMR resonances	undispersed and broad	relatively more dispersed and sharp

of the MG, suggestive of a significant hydrophobic core rather than patches of exposed and buried hydrophobic surfaces.

DISCUSSION

Alkali- and Acid-Denatured Forms of Cyt c. pH-denatured states are structurally not comparable with urea- or GdnHCl-unfolded states (*52*). However, how different are the acid- and base-denatured forms (U_A and U_B states, respectively)? Because these conformations represent starting points for the transitions to the corresponding MG states, a comparison of their structural features is essential. Unfortunately, a detailed comparison is not feasible with the limited results available for the U_B state. Table 1 lists a few properties based on the available data for the U_A state of ferricyt *c* (*12*, *53*−*56*) and results from this paper (Figures 1 and 2). Both states are maximally expanded but are different in terms of environmental polarity and water exposure of the fluorophore. The secondary structural content is similar. The NMR resonances for both U_A and U_B states are exchanged-broadened because of motions in the 100−1000 s^{-1} range, with the latter being relatively much slower (compare Figure 1 of ref *56* with Figure 2 of this paper). This qualitative sketch suggests relatively constrained dynamics for alkali-denatured cyt-CO, where the W59 indole and certain other side chains perhaps form apolar clusters. We also note that several control experiments, including NMR spectroscopy (data not shown), have indicated that the U_B state is monomeric and is stable for at least 9 h.

Alkali MG (B State) of Ferrocyt c. Results presented show that a MG state of ferrocyt *c* populates in the highly alkaline salt-containing aqueous medium. Transformation of the destabilized states of many proteins to MG-like forms by a wide variety of solution conditions, solvent additives, and cosolvents have been documented (*1*, *13*−*16*, *50*, *53*). All of these forms exhibit generally similar overall properties (*1*, *57*), although the mechanism of stabilization depends upon the specific action of the additive employed. Because ions fundamentally influence protein electrostatics, the mechanism of ion-induced stabilization of denatured proteins at both extremes of pH is expected to be the same. Judging by the pK_a values of ionizable groups of amino acids, the net charges of cyt *c* at pH <2 and pH >12.5 are +24 and −17, respectively. Under these conditions, the extrinsically added counterions can exert an effect on the protein by either reducing the electrostatic repulsion, direct binding to form ion pairs (*53*, *54*, *58*), or possibly both. When we look from this perspective, the acid MG state, extensively studied for a large number of proteins, including the paradigmatic "ferricyt *c*" (*12*, *53*−*56*), and the alkali MG state of "ferrocyt *c*" are expected to share at least qualitatively similar structural and dynamic properties. The molecular compactness and secondary-structure content of the alkali state observed here are qualitatively comparable with those reported for the acid MG state of ferricyt *c* (*12*, *56*, *59*, *60*; see Table 1). Certain other properties observed for the alkali MG form of ferrocyt *c*, however, do not concur with the generic prescription for the acid state. In the following, the customary labels "A" and "B" states will be used for the acid and alkali MG states, respectively.

Moderately Rigid Tertiary Structure in the B State of Ferrocyt c. The disordered nature or apparent absence of the tertiary structure is a hallmark of the MG state for all of the proteins studied (*1*, *5*). The B state of ferrocyt *c* however contains definite traces of tertiary interactions. For cyt *c*, the absence of the near-UV CD signal, as seen in the present study also (Figure 1f), is tacitly assumed to be an indication of the loss of the tertiary structure (*1*, *12*), while it does not need to always be so. The near-UV CD signal of cyt *c* originates from the rotational strength of the W59 side chain because of the coupling of its electric transition dipole moment with that of the heme group (*61*), and because the dipole interaction potential depends upon the geometric relationship between the two participating groups, the absence of the near-UV CD signal is a sure indication of a perturbation in the relative orientation and the distance between the two chromophores. It does not necessarily mean a general loss of the tertiary structure leading to an increased fluctuation and conformational averaging of the side chain. The NMR spectra (Figure 2) provide the most convincing evidence for the presence of some defined tertiary interactions. NaCl encourages the growth of a number of both aromatic and aliphatic resonances associated with tertiary interactions, and the observation of long-range NOE interactions strengthens the fact. The cooperativity observed for the GdnHCl-induced unfolding transition for the B state (Figure 5) also points to the presence of an ordered tertiary structure, because the steepness of denaturant-induced unfolding curves strongly depends upon the content of the rigid tertiary structure (*49*, *62*). Moderately rigid tertiary interactions, when present, as in the case of B states of ferrocyt *c* and β-lactamase (*17*), can not only contribute to molecular compaction but also result in restricted environmental averaging for the side chains as indicated by the fairly narrow NMR lines (Figure 2e).

Constrained Overall Dynamics in the U_B State of Ferrocyt c Induced by NaCl. Spatial displacement of thermal fluctuations and, hence, collisions between different groups of atoms

each exhibiting collective motions are dramatically reduced in the U_B state of ferrocyt *c*. The inference is drawn from the results of a set of specific experiments where we observe the rate constant for the association of CO with the alkaline ferrocyt *c* (k_{ass}). This reaction is not diffusion- or encounter-controlled. It rather involves substantial energy barrier or steric requirements, and hence, many collisions between the CO and protein groups, particularly the heme ring, are required before the reaction ensues. The value of k_{ass} under a given solution condition then depends upon the frequency of collisions involving the CO and heme side chains that exhibit highly collective motions (*63*). The rate constant for the CO association reaction, k_{ass}, decreases dramatically as the base-denatured polypeptide is held in the presence of increments of salt (Figure 3b). Accordingly, the activation energy for the reaction, E_a, also goes up (Figure 3d). In fact, in the presence of a sufficient NaCl concentration to fully populate the B state, values for both k_{ass} and E_a match those observed for the native state (parts b and d of Figure 3). Such hindered collective motions are not commonly associated with the U_A state. Because of dynamic disorder in the tertiary structure, the A state is known to be highly mobile (*64*) with low energetic barriers for conformational fluctuations in the millisecond time scale (*65*). The absence of nonhelical hydrogen bonds because of a high degree of disorder in the side chain of a majority of residues has been observed for the A state of ferricyt *c* (*55*, *56*). On the other hand, restricted mobility of aromatic side chains has also been reported for the A state of other proteins (*37*, *41*). The conclusion that the collective motions involving the side chains of the B state of ferrrocyt *c* are relatively restrained is consistent with the indications of an organized tertiary structure discussed above.

The dynamics of even the polypeptide backbone is highly controlled in the B state. This information is provided by intrachain diffusion rates extracted from laser photolysis of CO in the presence of different concentrations of NaCl (Figure 4). Because the diffusion rate in the alkali-denatured cyt-CO is minimally affected by salt, it is likely that any increase in the diffusion rate expected for a relatively compact B state is countered by growing stiffness of the polypeptide. Chain stiffness is uncharacteristic to dynamic properties of the MG state. Indeed, the polypeptide backbone in the A state is more mobile with respect to both native and unfolded states (*1*). A small but recognizable increase in the amplitude of local backbone fluctuations characterizes the transition from the acid-denatured state to the MG state of α-lactalbumin (*64*). Values of the NMR-measured backbone N−H order parameter, which provides an indication of the rigidity of the protein main chain, decrease significantly in the A state (*66*). Molecular dynamics simulations also show a substantial increase of the fluctuations in the main-chain dihedral angles φ and ψ (*67*). A molecular interpretation of the chain stiffness in the B state is unclear at present.

To summarize, the B state of ferrocyt *c* is distinguished by an appreciable level of ordered tertiary interactions, restrained collective motions that cover larger length scales, and a stiff backbone, and it shares with other MGs the common property of being compact and having similar secondary-structure content to the native state.

Stability of the B State of Ferrocyt c. The B state is expected to be sufficiently stable, because it is braced by a nativelike structural order, modest dynamics, and a compact molecular organization. The measured stability to unfolding by GdnHCl is 5.2 (±1) kcal mol^{-1} (Figure 5), substantially higher than the reported free energy of unfolding of MGs in water (*1*, *51*, *68*−*70*). Several nonstructural auxiliary factors can determine the energetic stability of MGs. For example, time-averaged internalization of any uncompensated charge can reduce the stability, because charge burial in the low dielectric protein interior is energetically not preferred. The charge on the heme group of cyt *c* itself provides an illustrative example. The ferricyt *c* A state has a mixed-spin ferric iron (*12*), meaning that a fraction of the A state molecules carries a +ve charge, whereas the charge on the persistent low-spin ferrous heme is 0 because of the pairing of all six d-orbital electrons. Thus, the A state of ferricyt *c* is less stable than the B state of ferrocyt *c*. Charge density in relation to protein motions can also play a role. High-frequency atomic fluctuations at the site of a protein charge can decrease the charge density by distorting the Debye−Huckel ion sphere, leading to a relatively weaker ion−protein interaction. The variable strength of the interaction of ions with the MG states of different proteins can explain the observed differences in stability.

In the context of stability, it is worthwhile considering the relative cooperativity of GdnHCl unfolding transitions of the A and B states. For GdnHCl unfolding of the A state of ferricyt *c* and several acetylated forms of the protein, Goto and co-workers report a m_g value of 1.85 kcal mol^{-1} M^{-1} (*54*). Apparently, the cooperativity of the unfolding transition is independent of the extent of acetylation. The corresponding value for the B state is 2.3 (±0.6) kcal mol^{-1} M^{-1} (Figure 5), which is fairly comparable. These comparisons suggest that the amount of solvent exposure of amino acid residues accompanying the unfolding of A and B states is similar. Thus, the two states appear equivalent in terms of the content of buried hydrophobic surfaces.

How Ordered Is the B State? MGs of different proteins are structurally different. Furthermore, even for a given protein, MGs stabilized by different conditions could be very different. For example, at least three structurally distinct A states each separated by significant energy barriers have been shown for staphylococcal nuclease (*71*, *72*). The two A states for ferricyt *c* have a similar secondary structure (*35*, *53*) but different molecular compactness (*24*). In general, MGs could be divided into three major classes: highly ordered, classical, and disordered. When the specific tertiary structure is taken as the orderly mark (*73*), the classical MGs that exhibit a reduced tertiary structure and increased fluctuations of side chains are between the highly ordered and disordered categories. In this perspective, the B state of cyt *c* could be described as an ordered MG, because it exhibits fairly ordered tertiary interactions. Considering the secondary-structure content for the description of structural order (*71*), the B state can be categorized as a highly ordered MG, because it retains near-native secondary structure and nearly half of the folding stability of the native state. Further experiments will be needed to show the possible existence of different forms of B states.

Is the B State a Short-Lived Postbarrier Intermediate in the Folding of Ferrocyt c? The classical view proposes that

the MG state represents a common early intermediate in the folding pathway of all proteins (*1*, *74*). Later advances in the field indicate that in some cases they correspond to late folding intermediates (*10*, *11*). Horse cyt *c* is an apparent two-state folder with no detectable accumulation of intermediates in both equilibrium and kinetic pathways (*28*). Kinetic studies have indicated that, because of a downhill-biased run in the postbarrier course of folding, the reaction coordinate shows no minima appreciably low in energy (*27*, *28*). However, the real-time NMR measurement of amide hydrogen exchange in the presence of subdenaturing concentrations of GdnHCl (*75*) and the native-state equilibrium hydrogen-exchange experiments developed by Englander and colleagues (*76*, *77*) have demonstrated the existence of short-lived nativelike intermediates, I_n, in the late or post-transition stages of folding. They are transient because no appreciable energy barrier separates them from the globally folded native state, and hence, they do not populate the kinetic pathway unless fortuitous barriers because of bad intramolecular contacts frustrate folding in the post-transition stages (*78*). As judged by its overall dynamics and structural organization, the B state studied in this paper may appear to match such a late short-lived intermediate. The preponderance of ordered tertiary interactions in the B state perhaps alleviates the energetically difficult process of side-chain packing in the late stages of folding. Ongoing kinetic studies will address these issues.

ACKNOWLEDGMENT

This paper is dedicated to the memory of Professor Oleg B. Ptitsyn with whom A. K. B. had held many discussions on the significance of the MG state in the protein-folding problem. A. K. B. is the recipient of a Swarnajayanti Fellowship from the Department of Science and Technology, Government of India.

REFERENCES

1. Ptitsyn, O. B. (1995) Molten globule and protein folding, *Adv. Protein Chem. 47*, 83−229.
2. Privalov, P. L. (1979) Stability of proteins. Small globular proteins, *Adv. Protein Chem. 33*, 167−241.
3. Privalov, P. L., and Khechinashvili, N. N. (1974) A thermodynamic approach to the problem of stabilization of globular protein structure. A calorimetric study, *J. Mol. Biol. 86*, 665−684.
4. Jackson, S. E., and Fersht, A. R. (1991) Folding of chymotrysin inhibitor 2. 1. Evidence for a two-state transition, *Biochemistry 30*, 10428−10435.
5. Kuwajima, K. (1989) The molten globule state as a clue for understanding the folding and coopertivity of globular-protein structure, *Proteins: Struct., Funct., Genet. 6*, 87−103.
6. Matthews, C. R. (1993) Pathways of protein folding, *Annu. Rev. Biochem. 62*, 653−683.
7. Evans, P. A., and Radford, S. E. (1994) Probing the structure of folding intermediates, *Curr. Opin. Struct. Biol. 4*, 100−106.
8. Wolynes, P. G., Onuchic, J. N., and Thirumalai, D. (1995) Navigating the folding routes, *Science 267*, 1619−1620.
9. Colón, W., and Roder, H. (1996) Kinetic intermediates in the formation of the cytochrome *c* molten globule, *Nat. Struct. Biol. 3*, 1019−1025.
10. Kuwajima, K., and Arai, M. (2000) The molten globule state: The physical and biological significance, in *Mechanism of Protein Folding* (Pain, R. H., Ed.) 2nd ed., pp 138−174, Oxford University Press, New York.
11. Mok, K. H., Nagashima, T., Day, I. J., Hore, P. J., and Dobson, C. M. (2005) Multiple subsets of side-chain packing in partially folded states of α-lactalbumins, *Proc. Natl. Acad. Sci. U.S.A. 102*, 8899−8904.
12. Ohgushi, M., and Wada, A. (1983) "Molten globule state": A compact form of globular proteins with mobile side-chains, *FEBS Lett. 164*, 21−24.
13. Bychkova, V. E., Dujsekina, A. E., Klenin, S. I., Tiktopulo, E. I., Uversky, V. N., and Ptitsyn, O. B. (1996) Molten globule like state of cytochrome *c* under conditions simulating those near the membrane surface, *Biochemistry 35*, 6058−6063.
14. Davis-Searles, P. R., Morar, A. S., Saunders, A. J., Erie, D. A., and Pielak, G. J. (1998) Sugar-induced molten globule model, *Biochemistry 37*, 17048−17053.
15. Moosavi-Movahedi, A. A., Chamani, J., Goto, Y., and Hakimelahi, G. H. (2003) Formation of the molten globule-like state of cytochrome *c* induced by *n*-alkyl sulfates at low concentrations, *J. Biochem. 133*, 93−102.
16. Uversky, V. N. (2002) Natively unfolded proteins: A point where biology waits for physics, *Protein Sci. 11*, 739−756.
17. Goto, Y., and Fink, A. L. (1989) Conformational states of β-lactamase: Molten globule states at acidic and alkaline pH with high salt, *Biochemistry 28*, 945−952.
18. Rami, B. R., and Udgaonkar, J. B. (2002) Mechanism of formation of a productive molten globule form of barstar, *Biochemistry 41*, 1710−1716.
19. Lambeth, D. O., Campbell, K. L., Zand, R., and Palmer, G. (1973) The appearance of transient species of cytochrome *c* upon rapid oxidation or reduction at alkaline pH, *J. Biol. Chem. 248*, 8130−8136.
20. Chalikian, T. V., Gindikin, V. S., and Breslauer, K. J. (1996) Spectroscopic and volumetric investigation of cytochrome *c* unfolding at alkaline pH: Characterization of the base-induced unfolded state at 25 °C, *FASEB J. 10*, 164−170.
21. Wilson, M. T., and Greenwood, C. (1996) in *Cytochrome c: A Multidisciplinary Approach* (Scott, R. A., and Mauk, A. G., Eds.) pp 611−634, University Science Books, Sausilito, CA.
22. Battistuzzi, G., Borsari, M., Loschi, L., Martinelli, A., and Sola, M. (1999) Thermodynamics of the alkaline transition of cytochrome *c*, *Biochemistry 38*, 7900−7907.
23. Nelson, C. J., and Bowler, B. E. (2000) pH dependence of formation of a partially unfolded state of a Lys 73 → His variant of iso-1-cytochrome *c*: Implications for the alkaline conformational transition of cytochrome *c*, *Biochemistry 39*, 13584−13594.
24. Cinelli, S., Spinozzi, F., Itri, R., Finet, S., Carsughi, F., Onori, G., and Mariani, P. (2001) Structural characterization of the pH-denatured states of ferricytochrome-*c* by synchrotron small-angle X-ray scattering, *Biophys. J. 81*, 3522−3533.
25. Hoang, L., Bédard, S., Krishna, M. M. G., Lin, Y., and Englander, S. W. (2002) Cytochrome *c* folding pathway: Kinetic native-state hydrogen exchange, *Proc. Natl. Acad. Sci. U.S.A. 99*, 12173−12178.
26. Bhuyan, A. K., and Udgaonkar, J. B. (2001) Folding of horse cytochrome *c* in the reduced state, *J. Mol. Biol. 312*, 1135−1160.
27. Prabhu, N. P., Kumar, R., and Bhuyan, A. K. (2004) Folding barrier in horse cytochrome *c*: Support for a classical folding pathway, *J. Mol. Biol. 337*, 195−208.
28. Kumar, R., and Bhuyan, A. K. (2005) Two-state folding of horse ferrocytochrome *c*: Analyses of linear free energy relationship, chevron curvature, and stopped-flow burst relaxation kinetics, *Biochemistry 44*, 3024−3033.
29. Santoro, M. M., and Bolen, D. W. (1988) Unfolding free energy changes determined by the linear extrapolation method. 1. Unfolding of phenylmethanesulfonyl α-chymotrypsin using different denaturants, *Biochemistry 27*, 8063−8068.
30. Bhuyan, A. K. (2002) Protein stabilization by urea and guanidine hydrochloride. *Biochemistry 41*, 13386−13394.
31. Kumar, R., Prabhu, N. P., Yadaiah, M., and Bhuyan, A. K. (2004) Protein stiffening and entropic stabilization in the subdenaturing limit of guanidine hydrochloride, *Biophys. J. 87*, 2656−2662.
32. Kumar, R., Prabhu, N. P., and Bhuyan, A. K. (2005) Ultrafast events in the folding of ferrocytochrome *c*, *Biochemistry 44*, 9359−9367.
33. Vanderkooi, J. M., and Erecinska, M. (1975). Cytochrome *c* interaction with membranes. Absorption and emission spectra and binding characteristics of iron-free cytochrome *c*, *Eur. J. Biochem. 60*, 199−207.
34. Tsong, T, Y. (1974) The Trp-59 fluorescence of ferricytochrome *c* as a sensitive measure of the over-all protein conformation, *J. Biol. Chem. 249*, 1988−1990.
35. Goto, Y., Calciano, L. J., and Fink, A. L. (1990) Acid-induced folding of proteins, *Proc. Natl. Acad. Sci. U.S.A. 87*, 573−577.

36. Ptitsyn, O. B. (1987) Protein folding: Hypothesis and experiments, *J. Protein. Chem. 6*, 273−293.
37. Dolgikh, D. A., Abaturov, L. V., Bolotina, I. A., Brazhnikov, E. V., Bychkova, V. E., Gilmanshin, R. I., Lebedev, O. Y., Semisotnov, G. V., Tiktopulo, E. I., and Ptitsyn, O. B. (1985) Compact state of a protein molecule with pronounced small-scale mobility: Bovine α-lactalbumin, *Eur. Biophys. J. 13*, 109−121.
38. Kuwajima, K., Harushima, Y., and Sugai, S. (1986) Influence of Ca^{2+} binding on the structure and stability of bovine α-lacalbumin studied by circular dichroism and nuclear magnetic resonance spectra, *Int. J. Peptide Protein Res. 27*, 18−27.
39. Baum, J., Dobson, C. M., Evans, P. A., and Hanley, C. (1989) Characterization of a partly folded protein by NMR methods: Studies on the molten globule state of guinea pig α-lactalbumin, *Biochemistry 28*, 7−13.
40. Alexandrescu, A. T., Evans, P. A., Pitkeathly, M., Baum, J., and Dobson, C. M. (1993) Structure and dynamics of the acid-denatured molten globule state of α-lactalbumin: A two-dimensional NMR study, *Biochemistry 32*, 1707−1718.
41. Dolgikh, D. A., Gilmanshin, R. I., Brazhnikov, E. V., Bychkova, V. E., Semisotnov, G. V., enyaminov, S. Y., and Ptitsyn, O. B. (1981) α-Lactalbumin: Compact state with fluctuating tertiary structure? *FEBS Lett. 136*, 311−315.
42. Bhuyan, A. K., and Kumar, R. (2002) Kinetic barriers to the folding of horse cytochrome *c* in the reduced state, *Biochemistry 41*, 12821−12834.
43. Theorell, H., and Åkesson, A. (1941) Studies on cytochrome *c*. II. The optical properties of pure cytochrome *c* and some of its derivatives, *J. Am. Chem. Soc. 63*, 1812−1827.
44. Jones, C. M., Henry, E. R., Hu, Y., Chan, C. K., Luck, S., Bhuyan, A., Roder, H., Hofrichter, J., and Eaton, W. A. (1993) Fast events in protein folding initiated by nanosecond laser photolysis, *Proc. Natl. Acad. Sci. U.S.A. 90*, 11860−11864.
45. Hagen, S. J., Hofrichter, J., Szabo, A., and Eaton, W. A. (1996) Diffusion-limited contact formation in unfolded cytochrome *c*: Estimating the maximum rate of protein folding, *Proc. Natl. Acad. Sci. U.S.A. 93*, 11615−11617.
46. Hagen, S. J., Latypov, R. F., Dolgikh, D. A., and Roder, H. (2002) Rapid intrachain binding of histidine-26 and histidine-33 to heme in unfolded ferrocytochrome *c*, *Biochemistry 41*, 1372−1380.
47. Jun, S., Bechhoefer, J., and Ha, B.-Y. (2003) Diffusion-limited loop formation of semiflexible polymers: Kramers theory and the intertwined time scales of chain relaxation and closing, *Europhys. Lett. 64*, 20−426.
48. Uversky, V. N., Semisotnov, G. V., Pain, R. H., and Ptitsyn, O. B. (1992) "All-or-none" mechanism of the molten globule unfolding, *FEBS Lett. 314*, 89−92.
49. Ptitsyn, O. B., and Uversky, V. N. (1994) The molten globule is a third thermodynamic state of protein molecules, *FEBS Lett. 341*, 15−18.
50. Qureshi, S. H., Moza, B., Yadav, S., and Ahmad, F. (2003) Conformational and thermodynamic characterization of the molten globule state occurring during unfolding of cytochromes-*c* by weak salt denaturants, *Biochemistry 42*, 1684−1695.
51. Pfeil, W. (1998) *Protein Stability and Folding: A Collection of Thermodynamic Data*, pp 17−343, Springer-Verlag, Berlin, Germany.
52. Tanford, C. (1968) Protein denaturation, *Adv. Protein Chem. 23*, 121−282.
53. Goto, Y., Takahashi, N., and Fink, A. L. (1990) Mechanism of acid-induced folding of proteins, *Biochemistry 29*, 3480−3488.
54. Hagihara, Y. Tan, Y., and Goto, Y. (1994) Comparison of the conformational stability of the molten globule and native states of horse cytochrome *c*: Effects of acetylation, heat, urea, and guanidine-hydrochloride, *J. Mol. Biol. 237*, 336−348.
55. Jeng, M.-F., Englander, S. W., Elöve, G. A., Wand, A. J., and Roder, H. (1990) Structural description of acid denatured cytochrome *c* by hydrogen exchange and 2D NMR, *Biochemistry 29*, 10433−10437.
56. Jeng, M.-F., and Englander, S. W. (1991) Stable submolecular folding units in a non-compact form of cytochrome *c*, *J. Mol. Biol. 221*, 1045−1061.
57. Arai, M., and Kuwajima, K. (2000) Role of the molten globule state in protein folding. *Adv. Protein Chem. 53*, 209−271.
58. Goto, Y., and Nishikori, S. (1991) Role of electrostatic repulsion in the acidic molten globule of cytochrome *c*, *J. Mol. Biol. 222*, 679−686.
59. Kataoka, M., Hagihara, Y., Mihara, K., and Goto, Y. (1993) Molten globule of cytochrome *c* studied by small-angle X-ray scattering, *J. Mol. Biol. 229*, 591−596.
60. Chalikian, T. V., Gindikin, V. S., and Breslauer, K. J. (1995) Volumetric characterizations of the native, molten globule, and unfolded states of cytochrome *c* at acidic pH. *J. Mol. Biol. 250*, 291−306.
61. Urry, D. W. (1965) Protein−heme interactions in heme-proteins, *Proc. Natl. Acad. Sci. U.S.A. 54*, 640−648.
62. Uversky, V. N., and Ptitsyn, O. B. (1996) All-or-none solvent-induced transitions between native, molten globule, and unfolded states in globular proteins, *Folding Des. 1*, 117−122.
63. Morgan, J. D., and McCammon, J. A. (1983) Molecular dynamics of ferrocytochrome *c*: Time dependence of the atomic displacements, *Biopolymers 22*, 1579−1593.
64. Chakraborty, S., Ittah, V., Bai, P., Luo, L., Haas, E., and Peng, Z. (2001) Structure and dynamics of the α-lactalbumin molten globule: Fluorescence studies using proteins containing a single tryptophan residue, *Biochemistry 40*, 7228−7238.
65. Kim, S., Bracken, C., and Baum, J. (1999) Characterization of millisecond time-scale dynamics in the molten globule state of α-lactalbumin, *J. Mol. Biol. 294*, 551−560.
66. Redfield, C., Smith, R. A. G., and Dobson, C. M. (1994) Structural characterization of a highly ordered molten globule at low pH, *Nat. Struct. Biol. 1*, 23−29.
67. Daggett, V., and Levitt, M. (1992) A model of the molten globule state from molecular dynamics simulations, *Proc. Natl. Acad. Sci. U.S.A.* 89, 5142−5146.
68. Ikeguchi, M., Kuwajima, K., Mitani, M., and Sugai, S. (1986) Evidence for the identity between the equilibrium unfolding intermediate and a transient folding intermediate: A comparative study of the folding reaction of α-lactalbumin and lysozyme, *Biochemistry 25*, 6965−6972.
69. Barrick, D., and Baldwin, R. L. (1993) The molten globule intermediate of apomyoglobin and the process of protein folding, *Protein Sci. 2*, 869−876.
70. Hagihara, Y., Aimoto, S., Fink, A. L., and Goto, Y. (1993) Guanidine hydrochloride-induced folding of proteins, *J. Mol. Biol. 231*, 180−184.
71. Uversky, V. N., Karnoup, A. S., Segel, D. J., Seshadri, S., Doniach, S., and Fink, A. L. (1998) Anion-induced folding of staphylococcal nuclease: Characterization of multiple equilibrium partially folded intermediates, *J. Mol. Biol. 278*, 879−894.
72. Nishimura, C., Riley, R., Eastman, P., and Fink, A. L. (2000) Fluorescence energy transfer indicates similar transient and equilibrium intermediates in staphylococcal nuclease folding, *J. Mol. Biol. 299*, 1133−1146.
73. Fink, A. L. (2005) Natively unfolded proteins, *Curr. Opin. Struct. Biol. 15*, 35−41.
74. Ptitsyn, O. B., Pain, R. H., Semisotnov, G. V., Zerovnik, E., and Razgulyaev, O. I. (1990) Evidence for a molten globule as a general intermediate in protein folding, *FEBS Lett. 262*, 20−24.
75. Bhuyan, A. K., and Udgaonkar, J. B. (1998) Stopped-flow NMR measurement of hydrogen exchange rates in reduced horse cytochrome *c* under strongly destabilizing conditions, *Proteins: Struct., Funct., Genet. 32*, 241−247.
76. Bai, Y., Sosnick, T. R., Mayne, L., and Englander, S. W. (1995) Protein folding intermediates: Native state hydrogen exchange, *Science 269*, 192−197.
77. Xu, Y., Mayne, L. C., and Englander, S. W. (1998) Evidence for an unfolding and refolding pathway in cytochrome *c*, *Nat. Struct. Biol. 5*, 774−778.
78. Rumbley, J., Hoang, L., Mayne, L., and Englander, S. W. (2001) An amino acid code for protein folding, *Proc. Natl. Acad. Sci. U.S.A. 98*, 105−112.

BI051882N